La radiologia medica (2018) 123:345–350
https://doi.org/10.1007/s11547-017-0845-4

CHEST RADIOLOGY

Analysis of CT features and quantitative texture analysis in patients with thymic tumors: correlation with grading and staging

Angelo Iannarelli[1] · Beatrice Sacconi[1] · Francesca Tomei[1] · Marco Anile[2] · Flavia Longo[3] · Mario Bezzi[1] · Alessandro Napoli[1] · Luca Saba[4] · Michele Anzidei[1] · Giulia D'Ovidio[1] · Roberto Scipione[1] · Carlo Catalano[1]

Received: 16 March 2017 / Accepted: 17 December 2017 / Published online: 6 January 2018

Abstract

Objectives To evaluate potential relationship between qualitative CT features, quantitative texture analysis (QTA), histology, WHO staging, Masaoka classification and myasthenic syndrome in patients with thymic tumors.

Materials and methods Sixteen patients affected by histologically proven thymic tumors were retrospectively included in the study population. Clinical information, with special regard to myasthenic syndrome and serological positivity of anti-AchR antibodies, were recorded. Qualitative CT evaluation included the following parameters: (a) location; (b) tumor edges; (c) necrosis; (d) pleural effusion; (e) metastases; (f) chest wall infiltration; (g) tumor margins. QTA included evaluation of "Mean" (M), "Standard Deviation" (SD), "Kurtosis" (K), "Skewness" (S), "Entropy" (E), "Shape from Texture" (TX_sigma) and "average of positive pixels" (MPP). Pearson–Rho test was used to evaluate the relationship of continuous non-dichotomic parameters, whereas Mann–Whitney test was used for dichotomic parameters.

Results Histological evaluation demonstrated thymoma in 12 cases and thymic carcinoma in 4 cases. Tumor necrosis was significantly correlated with QTA Mean ($p = 0.0253$), MPP ($p = 0.0417$), S ($p = 0.0488$) and K ($p = 0.0178$). WHO staging was correlated with Mean ($p = 0.0193$), SD ($p = 0.0191$) and MPP ($p = 0.0195$). Masaoka classification was correlated with Mean ($p = 0.0322$), MPP ($p = 0.0315$), skewness ($p = 0.0433$) and Kurtosis ($p = 0.0083$). Myasthenic syndrome was significantly associated with Mean ($p = 0.0211$) and MPP ($p = 0.0261$), whereas tumor size was correlated with Mean ($p = 0.0241$), entropy ($p = 0.0177$), MPP ($p = 0.0468$), skewness ($p = 0.009$) and Kurtosis ($p = 0.006$).

Conclusion Our study demonstrates significant relationship between radiomics parameters, histology, grading and clinical manifestations of thymic tumors.

Keywords Quantitative texture analysis · Computed tomography · Thymic neoplasm · Masaoka · WHO staging system

Introduction

The aim of radiomics is to evaluate the potential relationship between image and biological features of solid tumors [1] in order to access prognostic information before treatment and optimize therapeutic strategies. This approach has been recently applied to various tumors, such as glioblastoma [2–4], clear-cell renal carcinoma [5, 6], breast, rectal and lung adenocarcinoma [7–11]. Recent studies also demonstrated how quantitative texture analysis (QTA) may be used to complement conventional imaging features [12–17]; however, further investigations are needed to deepen the knowledge on the relationship between radiological and biological phenotypes and to enlarge the role of radiomics in clinical practice. The last National Cancer Institute (NCI) workshop report [1] proposed several fields of application

✉ Angelo Iannarelli
angelo.iannarelli@gmail.com

1 Department of Radiological, Oncological and Anatomopathological Sciences - Radiology, "Sapienza" University of Rome, Rome, Italy

2 Department of Thoracic Surgery, "Sapienza" University of Rome, Rome, Italy

3 Department of Radiological, Oncological and Anatomopathological Sciences - Oncology, "Sapienza" University of Rome, Rome, Italy

4 Department of Radiology, Azienda Ospedaliero Universitaria (A.O.U.), di Cagliari e Polo di Monserrato, Monserrato, Italy

for radiomics, identifying lung CT as the first research area in the priority list, but even less common lesions, such as thymic tumors, can represent interesting fields of application. The primary objective of this study was to evaluate the potential relationship between CT features, QTA data, histologic grading and tumor staging in patients with thymic tumors [18]; secondly, we assessed the ability of CT and QTA to predict the development of a myasthenic syndrome and serological positivity of anti-AchR antibodies.

Materials and methods

Patient population

This retrospective study received local Institutional Review Board approval; informed consent was obtained for all patients or relatives. Data from sixteen patients affected by thymic neoplasm were retrospectively retrieved from our local clinical database, according to the following inclusion criteria: (a) histologic diagnosis of thymic tumor obtained with percutaneous image-guided biopsy, mediastinoscopy or surgery; (b) tumor classification according to WHO and Masaoka systems; (c) CT scan data available for qualitative and QTA analysis; (d) no previous chemotherapy or radiation therapy; and (e) available clinical information including data on potential myasthenic syndrome and anti-AchR antibodies.

CT scan protocol

All CT scans were performed with a 64-slice CT scanner (SOMATOM Definition, Siemens, Forchheim—Germany) before and after intravenous administration of iodinated contrast agent (0.2 mg/kg of Iomeron 400 mgI/ml—Bracco SpA—Italy) in the venous phase (60 s delay after contrast injection). Images were acquired and reconstructed with the following parameters: tube rotation time 0.5 s, collimation 64 × 0.6, 1 and 3 mm slice thickness, reconstruction interval 1 and 3 mm, tube voltage 120 kV and tube current 200 mA.

Image analysis

Two radiologists with 8 years and 2 years of experience in chest CT, blinded to personal, clinical and histological data, independently performed a qualitative evaluation of the images. Any difference in interpretation was resolved with a consensus reading. QTA was performed by a third independent radiologist with 3 years of experience in advanced oncologic imaging.

Qualitative evaluation

The two observers were asked to evaluate qualitative CT features of thymic tumors, including: (a) location of the lesion, recorded as upper mediastinum and lower mediastinum (b) lesion edges, recorded as regular or irregular; (c) presence or absence of necrosis; (d) presence or absence of pleural effusion; (e) presence or absence of distant metastases; (f) infiltration of the chest wall, whether present or absent; and (g) lesion margins, described as sharp or irregular.

Quantitative texture analysis (QTA)

QTA was performed with TexRAD (TexRAD Ltd, Somerset, England, UK). Regions of interest (ROIs) were manually delineated around the thymic tumor on axial contrast-enhanced CT images, enclosing only tumor tissue [17, 19] as previously described. QTA included an image filtration-histogram technique followed by quantification of texture within the filtered images. The in-plane filtration step utilized a Laplacian of Gaussian spatial band-pass filter to produce a series of derived images highlighting features at different anatomic spatial scales varying from fine texture (SSF2, 2 mm in radius), medium texture (SSF3, 3 mm in radius) and coarse texture (SSF4, 4 mm in radius). Heterogeneity within ROIs (Fig. 1) was quantified with and without image filtration using the following histogram parameters, as previously described [20]:

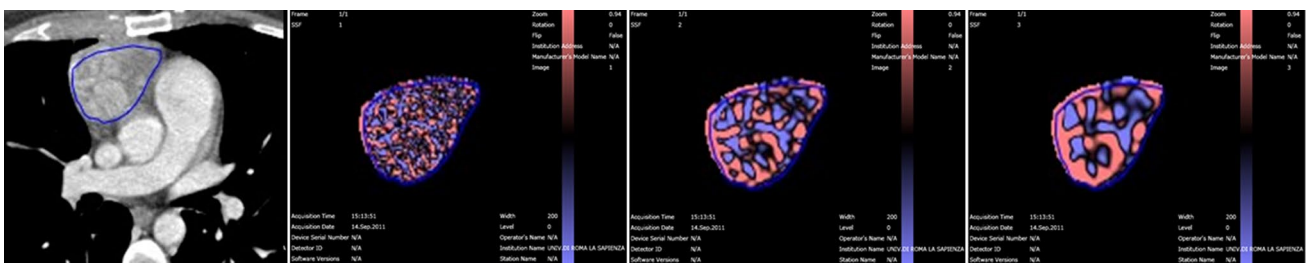

Fig. 1 ROI positioning on CECT and texture elaboration with different spatial scale filter (SSF): fine texture, medium texture and coarse texture

- Mean (M), which measures the average brightness in selected pixels.
- Standard deviation (SD), which measures variation or dispersion that exists from the mean.
- Kurtosis (K): from the Greek 'kyrtosis,' convexity, which measures peakedness and tailedness inversely related to the number of features highlighted (whether bright or dark); it increases by intensity variations in highlighted features.
- Skewness (S), which measures asymmetry in pixel distribution related to the average brightness of the highlighted features (predominantly bright features give positive values, predominantly dark objects give negative values); it tends to zero with increasing number of features highlighted and moves away from zero with density variation in highlighted features.
- Entropy (E), which measures texture irregularity in terms of randomness of gray-levels distribution inside the ROI.
- Shape from texture (TX_sigma): parameter dealing with information on the geometric surface of the lesion.
- MPP, average of positive pixels.

Statistical analysis

In this study, the normality of each continuous variable group was tested using the Kolmogorov–Smirnov Z test. Continuous data were described as the mean value ± SD, whereas non-continuous data with median and 2.5 and 97.5 percentiles. Spearman test was used to evaluate the correlation between QTA variables and WHO/Masaoka classification, MG and size. Mann–Whitney test was used for dichotomic parameters. A p value < 0.05 was regarded to indicate statistically significant association. All p values were calculated using a two-tailed significance level. R software (www.r-project.org) was employed for statistical analyses (version 3.1.3 "Smooth Sidewalk", R Foundation for Statistical Computing, Vienna, Austria).

Results

General results

Fifteen out of 16 patients underwent surgery; 1 patient was judged unresectable and therefore underwent chemotherapy. Histological examination demonstrated thymoma in 12 cases and thymic carcinoma in 4 cases. The average maximum diameter of the tumors was 54.43 mm (range 115–15 mm). According to the WHO score, patients were classified as follows: WHO B1: 1 patient; WHO B2: 7 patients; WHO B3: 4 patients; WHO C: 4 patients. According to the Masaoka staging system, patients were classified as follows: Masaoka I: 3 patients; Masaoka II: 7 patients; Masaoka III: 2 patients; Masaoka IV: 4 patients. Myasthenic syndrome was present in 7 out of 16 patients (5 WHO B2, 1 B3 and 1 C), with 6 of them being positive for anti-AchR antibodies; among the remaining 9 patients, one was positive for anti-AchR antibodies.

Qualitative analysis

Tumor location was in the upper mediastinum in 13 cases and lower mediastinum in 3 cases lesion. Lesion edges were regular in 15 patients and irregular in 1 patient. Tumor necrosis was present in 8 patients and absent in 8 patients. Pleural effusion was present in 3 patients and absent in 13 patients. Metastasis was present in 4 patients and absent in 12 patients. Infiltration of the chest wall was present in 1 patient and absent in 15 patients. Tumor margins were well defined in 13 patients and not defined in 3 patients. Due to the small sample size included in this preliminary study, necrosis was the only parameter which could be analyzed for relationship with the QTA data using the Mann–Whitney test, (Table 1).

Quantitative analysis

To assess whether the sample data analysis had a Gaussian trend, the Kolmogorov–Smirnov Z test was used (Table 2). Results derived from the relationship between quantitative parameters, staging systems and clinical features are summarized in Table 3; significant associations were observed between: WHO and mean ($p = 0.0193$), SD ($p = 0.0191$) and MPP ($p = 0.0195$) (Fig. 2); Masaoka and mean ($p = 0.0322$), MPP ($p = 0.0315$), skewness ($p = 0.0433$) and kurtosis ($p = 0.0083$) (Fig. 3). Myasthenic syndrome was significantly associated with mean ($p = 0.0211$) and MPP ($p = 0.0261$), whereas size was correlated with mean ($p = 0.0241$), entropy ($p = 0.0177$), MPP ($p = 0.0468$), skewness ($p = 0.009$) and kurtosis ($p = 0.006$) (Fig. 4).

Table 1 Mann–Whitney test results for relationship between QTA parameters and necrosis

Parameter	Mann–Whitney U test	Test Z
TX sigma	45	0.902
Mean	25	2.37
SD	32	1.77
Entropy	36	1.503
MPP	28	2.037
Skewness	29	1.97
Kurtosis	23	2.371
Total	25	2.204

Table 2 Kolmogorov–Smirnov *Z* test results

	Mean	95% CI	Median	95% CI	2.5–97.5 P	K–S zeta test
TX_sigma	1.037	0.983–1.092	1.033	0.978–1.089	0.819–1.314	0.8133
Mean	149.064	83.668–214.460	74.637	47.407–173.219	11.116–530.897	0.0278*
SD	175.778	142.058–209.499	162.24	114.804–213.059	78.912–325.260	0.399
Entropy	5.235	5.063–5.407	5.292	5.102–5.436	3.959–5.841	0.0001*
MPP	197.308	136.422–258.193	148.25	100.209–217.071	62.671–540.726	0.0334*
Skewness	1.34	0.917–1.763	1.274	0.658–1.974	− 0.411–3.685	0.5401
Kurtosis	6.482	3.546–9.417	4.416	3.001–10.130	− 0.0722–28.822	< 0.0001*
Total	1760.136	1010.320–2509.952	1069	433.764–2357.046	61.850–5017.000	0.146

Table 3 Pearson–Rho test results for relationship between quantitative parameters, staging systems and clinical features

		TX_sigma	Mean	SD	Entropy	MPP	Skewness	Kurtosis	Total
WHO	Rho value	− 0.321	− 0.495	− 0.495	0.12	− 0.494	0.212	0.33	0.23
	p value	0.1448	0.0193*	0.0191*	0.5961	0.0195*	0.3442	0.134	0.3028
Masaoka	Rho value	− 0.36	− 0.458	− 0.413	0.169	− 0.459	0.434	0.548	0.332
	p value	0.0999	0.0322*	0.0562	0.4509	0.0315*	0.0433*	0.0083*	0.1308
MG	Rho value	0.188	0.488	0.466	− 0.353	0.473	− 0.143	− 0.188	− 0.331
	p value	0.4025	0.0211*	0.0289*	0.1069	0.0261*	0.5262	0.403	0.1327
SIZE	Rho value	− 0.014	− 0.479	− 0.315	0.501	− 0.428	0.543	0.566	0.664
	p value	0.9503	0.0241*	0.1538	0.0177*	0.0468*	0.009*	0.006*	0.0007*

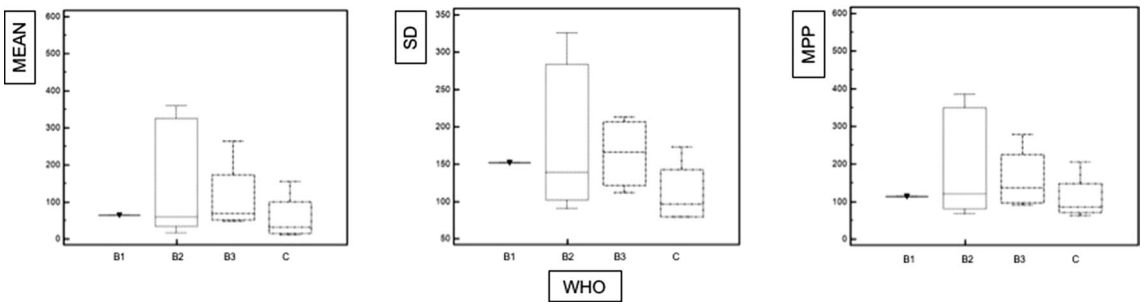

Fig. 2 Relationships data between QTA and WHO classification

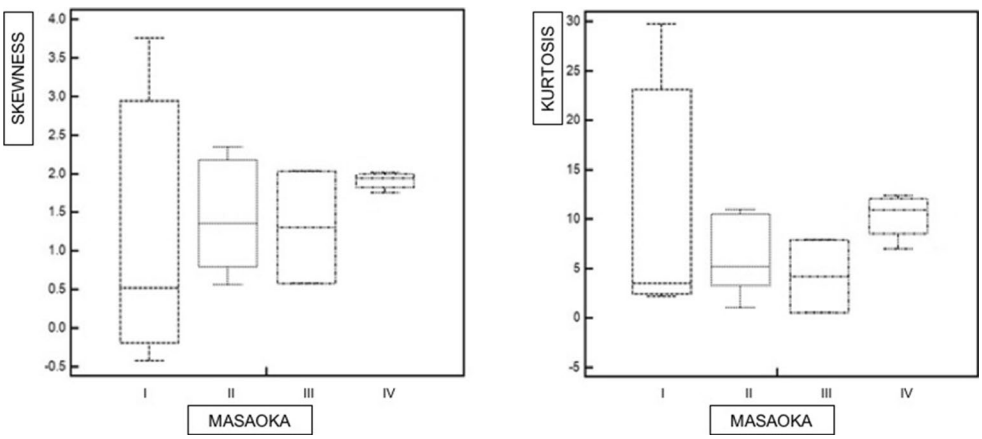

Fig. 3 Most significative relationship data between QTA and Masaoka staging system

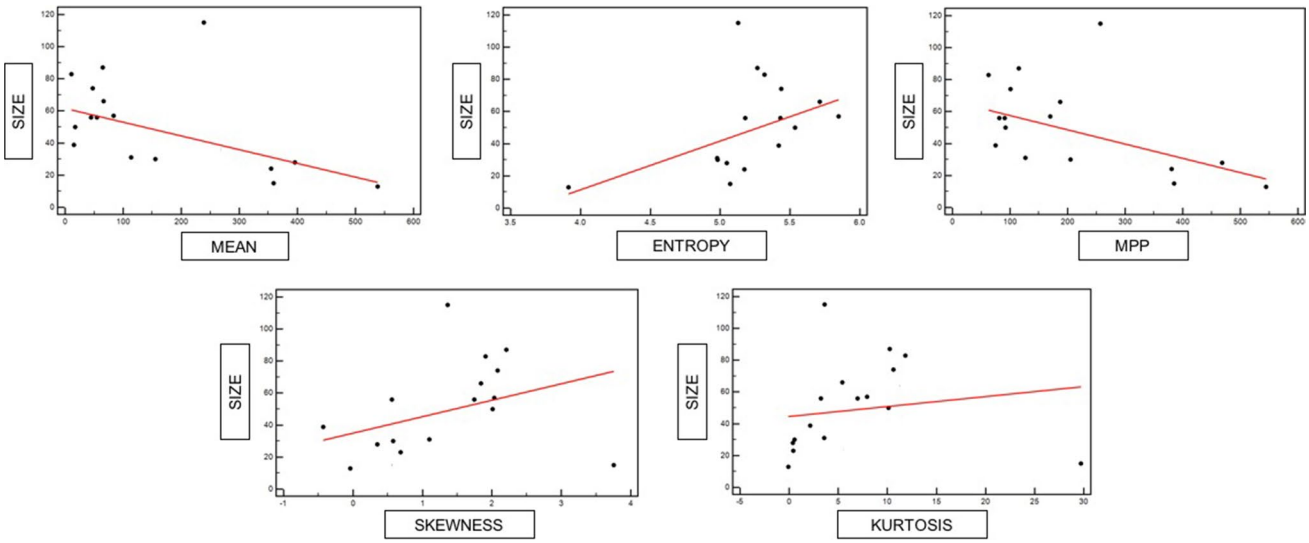

Fig. 4 Relationship data between QTA and lesion size

Discussion

The objective of this study was to evaluate the potential relationship of QTA with several clinical and imaging parameters in patients with thymic neoplasm. The identification of these relationships could derive noninvasive prognostic information before treatment and predict the occurrence of certain clinical scenarios, with possible impact on treatment decisions and patient management. Qualitative imaging features may represent immediate tools, potentially useful for the radiologist during reporting; unfortunately, in this preliminary study, the small number of patients enrolled allowed only a partial analysis, concerning only one qualitative parameter (necrosis). In particular, the association between necrosis and QTA parameters, such as kurtosis and skewness, was expected, since these two parameters represent the lack of homogeneity of the pixels and the deviation from normality, respectively. In any case, the finding of significant associations in this preliminary analysis looks promising; in the next future, a more extensive analysis including a higher number of patients and CT features is likely to reveal further associations. On the other hand, several significant relationships were demonstrated between QTA parameters, classification systems used for thymic lesions (WHO and Masaoka), tumor size and clinical condition; these associations can be explained basing on intrinsic features of tumors; for example, basing on entropy, whose values increase as size increases, we can infer that larger tumors have a less homogeneous pixel distribution; this observation is confirmed by the trend of MPP, which decreases with increasing tumor size, indicating a more homogeneous appearance in smaller tumors. These associations, particularly between QTA data and classification systems, seem also to indirectly suggest a relationship with prognosis, since these classifications have prognostic significance, especially the Masaoka system, already validated as independent prognostic factor [18]. Even in this case, the enrollment of more patients in a further study could allow a survival analysis, with the aim to assess the presence of an effective direct relationship between QTA parameters and clinical outcome. The relationship between QTA parameters and histology also represents an incentive for further studies, with the aim to correlate phenotypic and genotypic features of the tumor, as already done for other cancers, such as glioblastoma multiforme or lung adenocarcinoma. Furthermore, the ability to differentiate different components of the tumor through imaging analysis could also encourage the use of these techniques of radiomics and quantitative analysis as biopsy guidance, in order to identify the most suitable areas of the tumor to be sampled. Finally, the relationship between imaging data and the clinical scenario could confer the ability to predict the potential onset of symptoms and then to lead to a more straightforward patient management.

The greatest limitation of this work is represented by the small size of the examined sample: anyway, this in a preliminary study and these relationships need to be confirmed in larger studies, taking into account a larger number of patients and variables.

In conclusion, the identification of significant associations between radiological phenotype (including qualitative and quantitative evaluation), histological type, staging and clinical picture highlights the usefulness of this approach, whose main aim is to identify imaging features representing potential biological markers of the tumor, with consequent clinical and prognostic implications.

Funding No funding was received.

Compliance with ethical standards

Conflict of interest The authors declare that they have no conflict of interest.

Ethical approval All procedures performed in studies involving human participants were in accordance with the ethical standards of the institutional and/or national research committee and with the 1964 Helsinki declaration and its later amendments or comparable ethical standards.

Informed consent Informed consent was obtained from all individual participants included in the study.

References

1. Colen R, Foster I, Gatenby R, Giger ME, Gillies R, Gutman D, Heller M, Jain R, Madabhushi A, Madhavan S, Napel S, Rao A, Saltz J, Tatum J, Verhaak R, Whitman G (2014) NCI workshop report: clinical and computational requirements for correlating imaging phenotypes with genomics signatures. Transl Oncol 7(5):556–569
2. Jain R, Poisson LM, Gutman D, Scarpace L, Hwang SN, Holder CA, Wintermark M, Rao A, Colen RR, Kirby J, Freymann J, Jaffe CC, Mikkelsen T, Flanders A (2014) Outcome prediction in patients with glioblastoma by using imaging, clinical, and genomic biomarkers: focus on the nonenhancing component of the tumor. Radiology 272(2):484–493
3. Prasanna P, Patel J, Partovi S (2016) Radiomic features from the peritumoral brain parenchyma on treatment-naïve multiparametric MR imaging predict long versus short-term survival in glioblastoma multiforme: preliminary findings. Eur Radiol 27(10):4188–4197
4. Xi YB, Guo F, Xu ZL (2017) Radiomics signature: a potential biomarker for the prediction of MGMT promoter methylation in glioblastoma. J Magn Reson Imaging. https://doi.org/10.1002/jmri.25860
5. Karlo CA, Di Paolo PL, Chaim J, Hakimi AA, Ostrovnaya I, Russo P, Hricak H, Motzer R, Hsieh JJ, Akin O (2014) Radiogenomics of clear cell renal cell carcinoma: associations between CT imaging features and mutations. Radiology 270(2):464–471
6. Farber NJ, Kim CJ, Modi PK (2017) Renal cell carcinoma: the search for a reliable biomarker. ransl. Cancer Res 6(3):620–632
7. Rizzo S, Petrella F, Buscarino V, De Maria F, Raimondi S, Barberis M, Fumagalli C, Spitaleri G, Rampinelli C, De Marinis F, Spaggiari L, Bellomi M (2015) CT radiogenomic characterization of EGFR, K-RAS, and ALK mutations in non-small cell lung cancer. Eur Radiol 26(1):32–42
8. Buettner R, Wolf J, Thomas RK (2013) Lessons learned from lung cancer genomics: the emerging concept of individualized diagnostics and treatment. J Clin Oncol 31(15):1858–1865
9. Dehmeshki J, Amin H, Valdivieso M, Ye X (2008) Segmentation of pulmonary nodules in thoracic CT scans: a region growing approach. IEEE Trans Med Imaging 27(4):467–480. https://doi.org/10.1109/TMI.2007.907555
10. De Cecco CN, Ganeshan B, Ciolina M, Rengo M, Meinel FG, Musio D, De Felice F, Raffetto N, Tombolini V, Laghi A (2015) Texture analysis as imaging biomarker of tumoral response to neoadjuvant chemoradiotherapy in rectal cancer patients studied with 3-T magnetic resonance. Invest Radiol 50(4):239–245
11. Sacconi B, Anzidei M, Leonardi A (2017) Analysis of CT features and quantitative texture analysis in patients with lung adenocarcinoma: a correlation with EGFR mutations and survival rates. Clin Radiol 72(6):443–450
12. Lambin P, Rios-Velazquez E, Leijenaar R, Carvalho S, Stiphout RV, Granton P, Zeghers CM, Gillies R, Boellard R, Dekker A, Aerts HJ (2011) Radiomics: extracting more information from medical images using advance feature analysis. Eur J Cancer 48(4):441–446
13. Jaffe CC (2006) Measures of response: RECIST, WHO, and new alternatives. J Clin Oncol 24(20):3245–3251
14. Janssen MH, Ollers MC, van Stiphout RG, Riedl RG, van den Bogaard J, Buijsen J, Lambin P, Lammering G (2010) Blood glucose level normalization and accurate timing improves the accuracy of PET-based treatment response predictions in rectal cancer. Radiother Oncol 95(2):203–208
15. Rubin DL (2008) Creating and curating a terminology for radiology: ontology modeling and analysis. J Digit Imaging 21(4):355–362
16. Gonzales RC, Woods RE (2008) Digital image processing. Prentice Hall, Upper Saddle River
17. Chen CH, Pau LF, Wang PSP (eds) (1998) The handbook of pattern recognition and computer vision, 2nd edn. World Scientific Publishing Co., Singapore, pp 207–248
18. Venuta F, Anile M et al (2010) Thymoma and thymic carcinoma. Review. Eur J Cardio-Thorac Surg 37:13–25
19. Krishnan K, Ibanez L, Turner WD, Jomier J (2010) Avila RS. An open-source toolkit for the volumetric measurement of CT lung lesions. Opt Express 18(14):15256–15266
20. Boykov Y, Veksler O, Zabih R (2001) Fast approximate energy minimization via graph cuts. IEEE Trans Pattern Anal Mach Intell 23(11):1222–1239